第 43 卷 第 23 期/2023 年 12 月/光学学报 研究论文

光学学报

基于互相关的电光调制器相位标定方法

何思兴，陈友华，谢舜宇，匡翠方*

浙江大学光电科学与工程学院现代光学仪器国家重点实验室，浙江 杭州 310027

摘要 为了在使用相位电光调制器前能够快速准确地确定其半波电压，提出了一种基于频域互相关的干涉条纹相位差计算方法用于相位电光调制器的标定。该方法将条纹图像通过傅里叶变换转换成频谱图并对其进行滤波，将提取出的正负一级次频谱信息进行互相关操作，得到两张条纹图之间的相位差。为了验证所提方法在相位电光调制器标定中的作用，搭建实验系统，使得一路经过电光调制器的光与另一路光进行干涉后形成条纹像，改变电光调制器上施加的电压并用相机记录相位不同的干涉条纹，从而获得干涉条纹组，进而运用所提方法获得相位-电压对应关系。与轮廓法相比，所提方法快速且精度高。与迈克耳孙干涉法相比，该方法不需要重新搭建光路，操作迅速且能够达到相当的精度。

关键词 傅里叶光学；信号处理；频谱分析；相共轭；互相关；电光调制器

中图分类号 O436 **文献标志码** A **DOI**：10.3788/AOS231057

1 引 言

电光调制器(EOM)作为一种可以改变入射光相位和偏振态的器件，在诸多领域中都有广泛的应用，如光通信[1-3]、集成光学[4-7]和超分辨显微成像[8-10]等。电光调制器具有响应速度快、可靠等优势；但是由于电光调制器设备之间的差异，在实际操作中加载电压和变化的相位之间的关系与技术手册上的对应关系并不一致，且电光调制器工作在不同波长时对其加相同电压有着不同的相位变化。因此，在使用前需要对电光调制器的相位变化与电压变化的关系进行标定，因为其调制是线性的，只需要求相位变化与电压变化关系的斜率即可用于后续的实验。

常见的标定方法有轮廓法和迈克耳孙干涉法[11]。一些在波片中测定相位差的方法[12-14]因其光路和处理方法不适用，很少在电光调制器的标定中使用。轮廓法使用两条光路进行干涉，其中一路通过电光调制改变相位，按照一定的电压间隔拍摄干涉条纹，将两条条纹之间的位移除以条纹周期再乘以 2π 即得到相位差，再将相位差结合电压间隔即可求得半波电压，这种方法简单但是需要反复调整修正，费时费力，同时受相机像素的限制，精度有所降低。迈克耳孙干涉法将一个干涉臂通过电光调制器，通过施加电压使其产生移相后，再通过移动此臂改变光程差，以使干涉条纹消失，进而确定相位差，此方法的精度很高但是需要重新搭建光路并且比较耗时。

为了能够在不重新搭建光路的情况下快速准确地标定电光调制器的半波电压，研究了一种通过在频域中用前一张干涉条纹高级次频谱的复共轭与后一张条纹高级次频谱相乘计算相位差的互相关方法来标定半波电压的方法。使用该方法标定了超分辨显微成像系统中的电光调制器并将结果与迈克耳孙干涉法得到的结果进行对比，验证了该方法的准确性和可行性。

2 互相关法条纹相位差计算

2.1 互相关法原理

本研究使用多张条纹图像两两之间的互相关函数的相位角来确定相位差，较大程度地提高了条纹相位差的计算精度。

条纹照明强度函数为

$$I_n = 1 + \frac{m}{2}\cos(\boldsymbol{k}_0 \cdot \boldsymbol{r} + \varphi_n), \tag{1}$$

式中：m 为调制强度；$\boldsymbol{k}_0$ 为条纹的空间频率矢量，分布在照明平面上；$\boldsymbol{r}$ 为照明平面坐标系坐标；φ_n 为条纹的初相位。相机采集到的图像经过傅里叶变换转换到频域中后，得到条纹照明图像的频谱为

$$\tilde{D}_n = \tilde{h}(\boldsymbol{k})\left[\tilde{g}(\boldsymbol{k}) + \frac{m}{2}\mathrm{e}^{\mathrm{i}\varphi_n}\tilde{g}(\boldsymbol{k}-\boldsymbol{k}_0) + \frac{m}{2}\mathrm{e}^{-\mathrm{i}\varphi_n}\tilde{g}(\boldsymbol{k}+\boldsymbol{k}_0)\right], \tag{2}$$

收稿日期：2023-05-29；**修回日期**：2023-07-30；**录用日期**：2023-08-30；**网络首发日期**：2023-09-10

基金项目：国家重点研发计划(2021YFF0700302)、国家杰出青年科学基金(62125504)、国家自然科学基金(61975188)、浙江省自然科学基金(LY23F050010，LQ23F050010)

通信作者：*cfkuang@zju.edu.cn

式中：$\boldsymbol{k}$为像的空间频率矢量；$\tilde{h}(\boldsymbol{k})$为系统的光学传递函数；$\tilde{g}(\boldsymbol{k})$为照明样品频谱。对于条纹的频谱图来说，$\tilde{g}(\boldsymbol{k})\approx\delta(\boldsymbol{k})$[$\delta(\boldsymbol{k})$为冲激函数]，因此频谱图会在$\boldsymbol{k}=0$和$\boldsymbol{k}=\pm\boldsymbol{k}_0$处有三个峰值，运用掩模版将+1级或−1级处的频谱提取出来，此处提取±1级不会影响最终的结果，因为相位差的正负与选取的高级次的方向是一一对应的，而高级次在方向上是对称的，因此选取级次的不同只带来正负号上的差异并且条纹因相位变化移动的方向可以确定。在此以+1级来说明算法，因为0级和−1级的影响很小，+1级处的局部频谱近似为

$$\tilde{D}_n^{(+1)}=\tilde{h}(\boldsymbol{k})\frac{m}{2}\mathrm{e}^{\mathrm{i}\varphi_n}\tilde{g}(\boldsymbol{k}-\boldsymbol{k}_0)。\tag{3}$$

将第n个图像的第一级频谱共轭与第$n+1$个图像的第一级频谱相乘，可以得到相邻两张图的互相关函数为

$$\left[\tilde{D}_n^{(+1)}\right]^*\cdot\tilde{D}_{n+1}^{(+1)}=\frac{m^2}{4}\mathrm{e}^{\mathrm{i}(\varphi_{n+1}-\varphi_n)}\left|\tilde{h}(\boldsymbol{k})\tilde{g}(\boldsymbol{k}-\boldsymbol{k}_0)\right|^2,\tag{4}$$

式中：*代表复共轭。式(4)中，只有$\mathrm{e}^{\mathrm{i}(\varphi_{n+1}-\varphi_n)}$具有幅角信息，因此只要求出互相关函数的角度便可以得到两幅相邻图像的相位差。最终得到的相位差为

$$\Delta\varphi=\arctan\frac{\mathrm{Im}\left[\sum\limits_{\boldsymbol{k}}\frac{m^2}{4}\mathrm{e}^{\mathrm{i}(\varphi_{n+1}-\varphi_n)}\left|\tilde{h}(\boldsymbol{k})\tilde{g}(\boldsymbol{k}-\boldsymbol{k}_0)\right|^2\right]}{\mathrm{Re}\left[\sum\limits_{\boldsymbol{k}}\frac{m^2}{4}\mathrm{e}^{\mathrm{i}(\varphi_{n+1}-\varphi_n)}\left|\tilde{h}(\boldsymbol{k})\tilde{g}(\boldsymbol{k}-\boldsymbol{k}_0)\right|^2\right]}。\tag{5}$$

2.2　仿真验证

为验证该方法计算相位差的准确性，使用Matlab生成的条纹图进行仿真验证。图1为生成的6张条纹图像，每张图像大小为512×512，在像素单位下，$k_x=-21.6949$，$k_y=10.5133$，相位差设定为$\pi/7$，对于每张图片都施加均值为0、方差为0.2的高斯噪声。

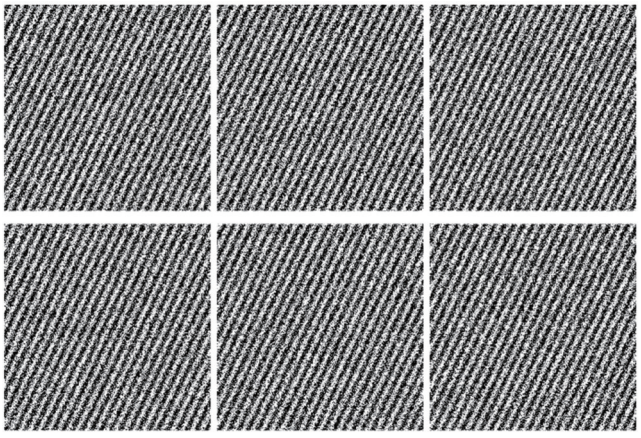

图1　Matlab生成的6张仿真条纹图像

Fig. 1　Six simulated stripe images generated by Matlab

通过Matlab的最值定位函数，找到各个频谱图中的除中心零频极大值外的极大值，用一个15×15大小的掩模将其截出，得到了图2所示的频谱图。

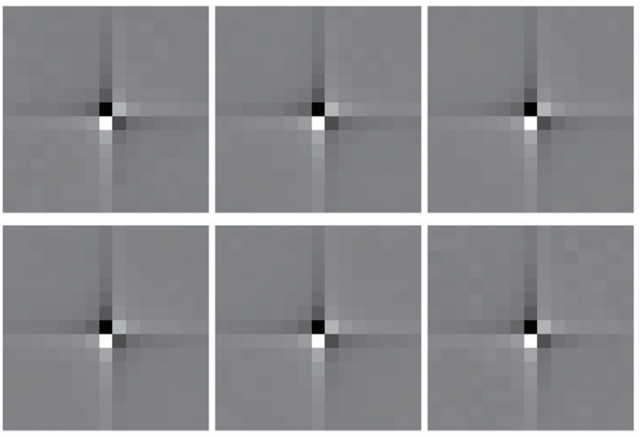

图2　图1中对应条纹的+1级或−1级频谱掩模截取图

Fig. 2　+1 order or −1 order spectrum mask screenshots corresponding to stripes in Fig. 1

根据式(4)，对图2中相邻的两幅图进行处理，最后使用Matlab自带的求相位的函数求出相位差。为了减小误差，将所得到的5个结果求均值，得到最终的相位差，因为相位变化是线性的，此相位差可以应用到每两张图像中间。最终求得的相位差为0.4489 rad，与$\pi/7\approx0.4487$rad的误差为0.0002 rad，可以看到本方法精度很高，足以对条纹相位差进行标定。

3　电光调制器标定及结果对比

3.1　电光调制器标定及结果

将本方法应用于电光调制器的标定中，确定改变相位与施加电压的关系。图3为标定电光调制器所用系统实物图。

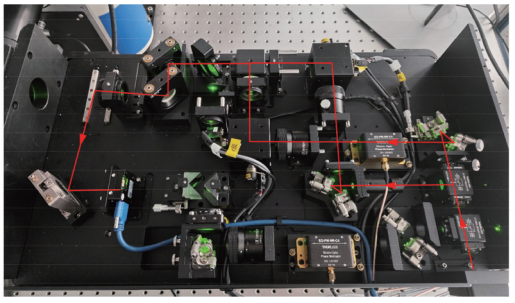

图3　标定电光调制器所用系统实物图(所用到的光路用带箭头的线标出)

Fig. 3　Picture of system used to calibrate electro-optical modulator (optical path used is marked by lines with arrows)

实验标定所用的光路为结构光照明超分辨显微成像系统的一部分，此系统基于电光调制器和振镜实现高速的成像[15]。图3中用线段标出的部分为结构光照明显微(SIM)系统的边缘光路，其中一条通过相位电光调制器，另一条不通过，最终两光束通过反射镜在大恒VEN-505-36U3M-M05相机处交会、干涉后形成条纹，图4为本实验中使用的光路简化图。

实验通过计算机控制采集卡给电光调制器施加电

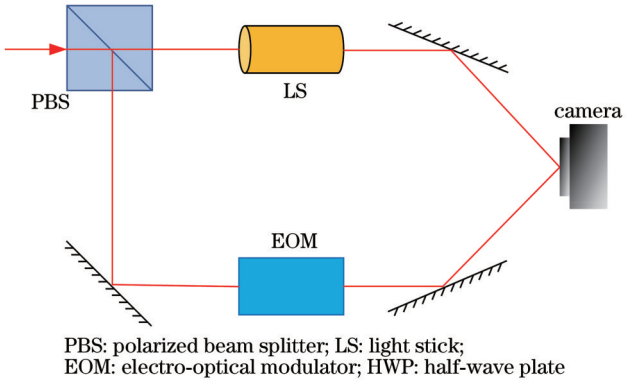

图 4　标定系统光路简化结构

Fig. 4　Simplified structure of optical path of calibration system

压，电压间隔为 1 V，电压范围为－10～9 V，每变换一次电压控制相机采集一幅图像并保存，共采集 20 幅等间隔位移的干涉条纹图像，每幅图像的大小为 512 pixel × 512 pixel。程序读入保存的图片后，将图片通过傅里叶变换转为频谱和频域幅度谱，条纹图频谱有三个级次。使用幅度谱寻找此时频谱中的强度最大点（条纹图的强度最大点为中心 0 级），为了寻找带有相位信息的高级次，使用值为 0 的掩模在不影响高级次的情况下将 0 级去除。

在去除了 0 级次的频谱图中寻找幅值最大的位置，此时为＋1 级或－1 级，在 2.1 节中所述级次的选择不会影响最终的结果，因此以＋1 级为例进行论述。以＋1 级所在位置为中心使用不包含 0 级位置大小的掩模将＋1 级频谱提取出来，接下来通过将提取出的高级次频谱中前一张频谱的复共轭与后一张频谱相乘做互相关处理，求出来的结果是一个复矩阵，将其全部元素相加，这时其复角度完全来源于两张图片的相位差，因此只需要求其角度即可得到相位差，将所有图片的相位差都求出来后取平均，即可消掉部分噪声抖动等的干扰，得到最终的相位差值。因为电压间隔是 1 V，因此 EOM 标定的半波电压可以表示为 $V_\pi=\pi/\Delta\varphi$。上述计算流程如图 5 所示。

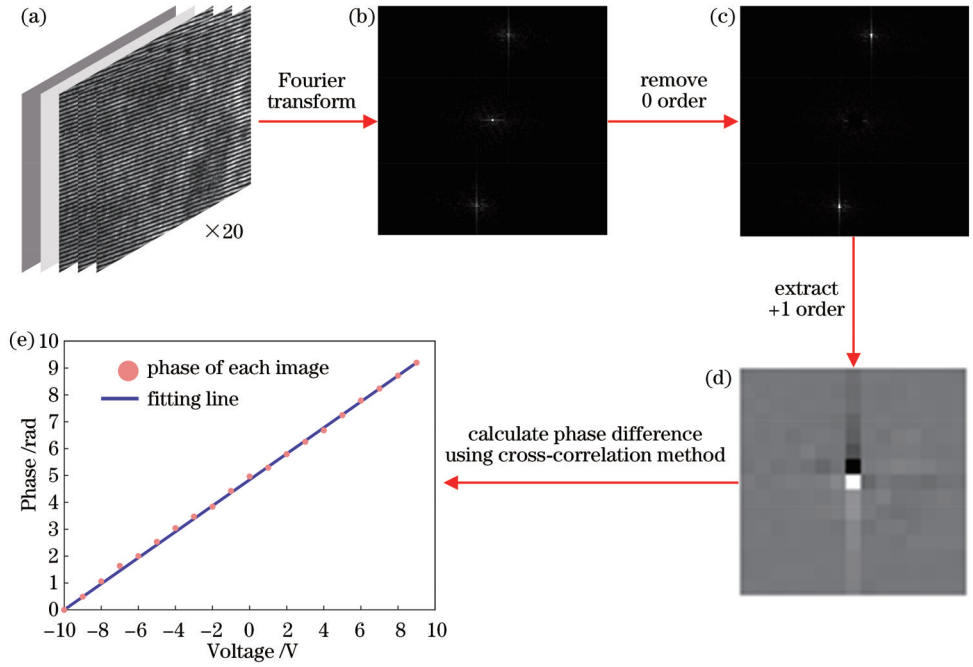

图 5　相位差计算流程图。(a)20 张拍摄的条纹图；(b)傅里叶频谱图；(c)去掉中心 0 级的频谱图；(d)提取出的＋1 级频谱；(e)互相关计算的各条纹相对相位及相位-电压的拟合直线

Fig. 5　Flow chart of phase difference calculation. (a) 20 fringe images; (b) Fourier spectrum; (c) spectrum with 0 order removed in center; (d) extracted ＋1 order spectrum; (e) relative phase of each image calculated by cross-correlation calculation and phase-voltage fitting line

使用 640 nm 和 561 nm 激光对其进行标定，并且以迈克耳孙干涉法的标定结果作为正确结果进行准确性的考量。为了能够进一步消除干扰所带来的误差，使用每个波段的激光各拍摄了 9 组如图 5 所示的 20 张条纹图，并将 9 组结果的平均值与准确标定值进行对比，结果如图 6 所示。

使用迈克耳孙干涉法标定得到的 640 nm 波段的半波电压为 6.6 V，使用本方法得到的结果为 6.57 V，二者相差 0.03 V，误差为 0.45%。使用迈克耳孙干涉法标定得到的 561 nm 波段的半波电压为 5.87 V，使用本方法得到的结果为 5.84 V，二者相差 0.03 V，误差为 0.51%。将误差换算为相位差的话，计算得到 640 nm 波段处的相位差为 0.478 rad，标准相位差为 0.476 rad，相差为 0.002 rad，561 nm 波段处的相位差

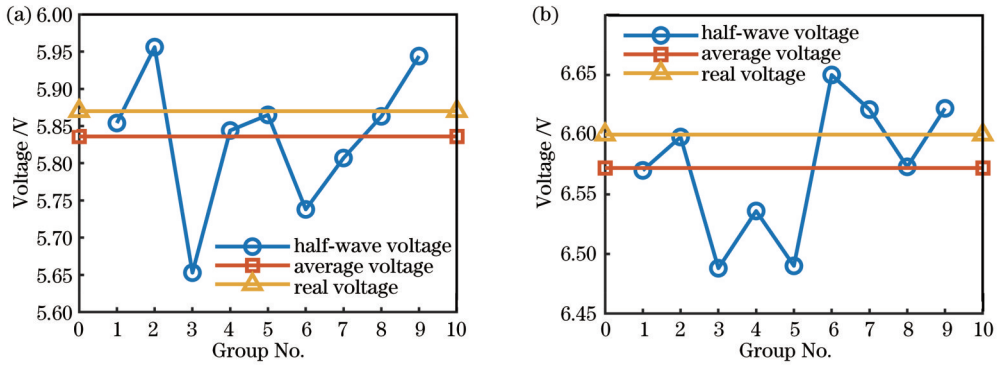

图 6　计算结果与标准值对比图。(a)640 nm 激光结果;(b)561 nm 激光结果

Fig. 6　Comparison of calculated results and standard values. (a) Results for 640 nm laser; (b) results for 561 nm laser

为 0.538 rad,标准相位差为 0.535 rad,相差为 0.003 rad。两者结果相对于仿真阶段 0.0002 rad 的误差,精度都有所下降,其原因在于实验过程中不可避免的抖动、条纹对比度相对较低以及噪声的存在等。实验中所用的光学平台和相机均为较低层次的设备,在精度方面都会造成不可避免的影响,但是本方法所测相位差相比于迈克耳孙干涉法所测相位差、SIM 系统在 2π 区间内三步相移或五步相移的相位变化已经可以忽略不计,对成像结果不会造成影响,因此该精度在标定结果的接受范围之内。

3.2　与轮廓法的精度对比

使用轮廓法对 3.1 节中获得的干涉条纹随电压移动的图像组进行处理,如图 7 所示。选取 640 nm 拍摄的一组图片中前 6 张图像,每张条纹的间隔电压为 1 V,选取一列像素的灰度值进行处理,如图 7(a)所示。图 7(b)所示为每张图像相同列的灰度值中部分像素的比较,可以看到条纹之间发生位移,选取图 7(b)线框部分的最低点进行相位差的测定,所测得的位置与电压的对应关系如图 7(c)所示,可以看出电压变化相同的情况下最低点偏移相同的距离。电压每变化 1 V,条纹偏移 1 pixel,而 1 个周期占据 12 pixel,设 1 V 电压变化量为 x,周期像素为 T,半波电压为 $T/2x$,根据轮廓法计算出的半波电压为 6 V,而本文方法得出的半波电压为 6.57 V,与迈克耳孙干涉法得到的 6.6 V 更加接近,因

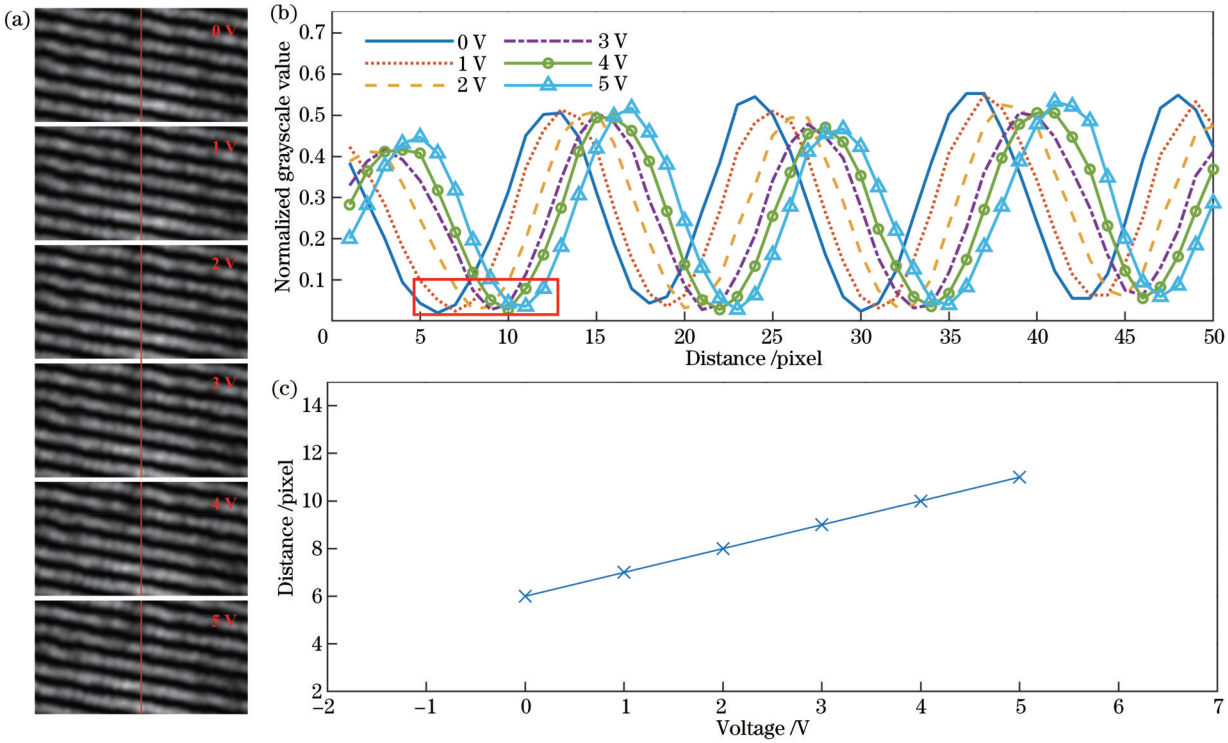

图 7　轮廓法测量得到的条纹相位差图。(a)电光调制器在不同电压下生成的条纹图;(b)图 7(a)中划线部分归一化灰度值分布图(部分显示);(c)图 7(b)线框中最低点位置图

Fig. 7　Phase difference of fringes measured by contour method. (a) Fringes generated by electro-optic modulator at different voltages; (b) distribution of normalized grayscale value in underlined portion in Fig. 7(a); (c) position of lowest points in wireframe in Fig. 7(b)

此本文方法精度更高且速度更快。

4 结 论

在使用电光调制器之前往往需要对其半波电压进行标定，以往使用的方法如迈克耳孙干涉法需要额外搭建光路，并且标定过程缓慢，标定过程容易受到噪声抖动等的干扰，轮廓法则精度不够高。因此提出了一种基于干涉条纹频域高级次互相关的方法来计算条纹图像之间的相位差，从而对电光调制器的半波电压进行标定。

该方法使用特定的掩模去除0级频谱并将高级次频谱提取出来，通过将前一张的高级次频谱的复共轭与后一张的高级次频谱相乘求角度继而求解相位差，仿真中相位误差达到0.0002 rad，实际检测中相位误差达到0.002 rad，半波电压误差为0.03 V，精度满足电光调制器标定需求。本方法的标定速度很快，不需要重新搭建光路，因此可以随时检验电光调制器是否发生漂移，从而确定是否需要进行修正。

在条纹频率较低的情况下，中心0级频谱会对边缘高级次频谱产生影响，简单的消除中心频谱依然会导致计算误差，因此未来选择先分离频谱再进行计算的方法或许会进一步提高精度。另外，在电光调制器的标定过程中，通过人为控制干涉光束之间的角度，可控制形成的条纹的频率，通过提高条纹频率可以消除这类影响，同时在条纹形态较好的情况下，中心频率对高频部分造成的影响已经十分微小，因此这部分的干扰可以进一步排除。

参 考 文 献

[1] Tibaldi A, Ghomashi M, Bertazzi F, et al. Organic electro-optic Mach-Zehnder modulators: from physics-based to system-level modeling[J]. Physica Status Solidi (a), 2021, 218(21): 2100390.

[2] Stenger V, Toney J, Brown D, et al. Single-sideband thin film lithium niobate (TFLN™) electro-optic modulators for RF over fiber[C]//Optical Fiber Communication Conference, March 11-15, 2018, San Diego, California. Washington, DC: Optica Publishing Group, 2018: M2I.5.

[3] Xu M, Tong S F, Wang D S. Automatic bias control system of high speed electro-optic modulator in DPSK Systems[J]. Proceedings of SPIE, 2015, 9522: 95220T.

[4] Wang Y, Liu T T, Liu J Y, et al. Organic electro-optic polymer materials and organic-based hybrid electro-optic modulators[J]. Journal of Semiconductors, 2022, 43(10): 101301.

[5] Feng S, Xue B. Micro-nano electro-optic modulator structure based on the Si/SiGe/Si material[J]. Journal of Nanoelectronics and Optoelectronics, 2020, 15(6): 693-699.

[6] Han H P, Xiang B X. Integrated electro-optic modulators in *x*-cut lithium niobate thin film[J]. Optik, 2020, 212: 164691.

[7] Rivera L C, Zaldivar-Huerta I, Juarez-Garcia A, et al. Electro-optic modulators for high-frequency telecommunications in integrated optic technology[J]. Proceedings of SPIE, 2001, 4419: 358-362.

[8] Urban B E, Xiao L, Chen S Y, et al. *In vivo* superresolution imaging of neuronal structure in the mouse brain[J]. IEEE Transactions on Biomedical Engineering, 2018, 65(1): 232-238.

[9] Urban B E, Yi J, Chen S Y, et al. Super-resolution two-photon microscopy via scanning patterned illumination[J]. Physical Review E, 2015, 91(4): 042703.

[10] 匡翠方, 谢舜宇, 陈友华, 等. 一种实现超高速结构光照明显微成像的方法和装置: CN115327757A[P]. 2022-11-11.
Kuang C F, Xie S Y, Chen Y H, et al. A method and device for realizing ultra-high-speed structured illumination microscopy imaging: CN115327757A[P]. 2022-11-11.

[11] 任洪亮, 王久扬, 楼立人, 等. 利用迈克耳孙干涉仪测量波片相位延迟量和快轴方向[J]. 中国激光, 2008, 35(2): 249-253.
Ren H L, Wang J Y, Lou L R, et al. Measuring phase retardation and fast axis azimuth of a wave plate using Michelson interferometer[J]. Chinese Journal of Lasers, 2008, 35(2): 249-253.

[12] 曾婧潇, 洪羽剑, 卢钧胜, 等. 液晶空间光调制器相位调制特性的快速测量与标定方法[J]. 光学学报, 2023, 43(3): 0312004.
Zeng J X, Hong Y J, Lu J S, et al. Fast measurement and calibration method for phase modulation characteristics of liquid-crystal spatial light modulator[J]. Acta Optica Sinica, 2023, 43(3): 0312004.

[13] 张敏娟, 李春阳, 李晋华, 等. 具有相位补偿的级联调制型相位延迟量精确检测方法[J]. 激光与光电子学进展, 2023, 60(1): 0112001.
Zhang M J, Li C Y, Li J H, et al. Accurate detection method of cascade modulation phase delay with phase compensation[J]. Laser & Optoelectronics Progress, 2023, 60(1): 0112001.

[14] 陈强华, 关裕, 周胜, 等. 基于双频激光干涉相位检测的高精度波片测量[J]. 光学学报, 2023, 43(1): 0112002.
Chen Q H, Guan Y, Zhou S, et al. High-accuracy wave plate measurement based on dual-frequency laser interferometry and phase detection[J]. Acta Optica Sinica, 2023, 43(1): 0112002.

[15] Xu F H, Zhang J C, Ding D D, et al. Real-time reconstruction using electro-optics modulator-based structured illumination microscopy[J]. Optics Express, 2022, 30(8): 13238-13251.

Phase Calibration Method of Electro-Optic Modulator Based on Cross-Correlation

He Enxing, Chen Youhua, Xie Shunyu, Kuang Cuifang*

State Key Laboratory of Modern Optical Instrumentation, College of Optical Science and Engineering, Zhejiang University, Hangzhou 310027, *Zhejiang, China*

Abstract

Objective Electro-optic modulators can change the phase and polarization state of incident light, therefore having a wide range of applications in many fields, such as optical communication, integrated optics, and super-resolution microscopy. They feature fast response and reliability. However, due to the differences among electro-optic modulator devices, the relationship between the applied voltage and the phase change in actual operation is not consistent with the corresponding relationship in the technical manuals. Meanwhile, when modulators are working at different wavelengths, applying the same voltage to the modulator results in different phase changes. Therefore, before utilization, it is necessary to calibrate the relationship between the phase change and voltage change of the electro-optic modulator. Since its modulation is linear, the slope of the function only needs to be obtained for subsequent experiments.

Common calibration methods include the contour method and the Michelson interferometry method. The contour method employs two optical paths for interference, one of which passes through an electro-optic modulator to change the phase. Interference fringes are taken at a certain voltage interval. The displacement between two fringes is divided by the fringe period and then multiplied by 2π to obtain the phase difference which is combined with the voltage interval to get the half-wave voltage. This method is simple but requires repeated adjustment and correction, which is time-consuming and laborious. Additionally, the limitation of camera pixels reduces the accuracy. The Michelson interferometry method passes one of the interferometer arms through an electro-optic modulator, applies a voltage to produce a phase shift, and then moves this arm to change the optical path difference and make the interference fringes disappear to determine the phase difference. This method has high accuracy but requires optical path rebuilding with too much consumed time.

To quickly and accurately calibrate the half-wave voltage of an electro-optic modulator without rebuilding an optical path, we study a method using cross-correlation in the frequency domain. The complex conjugate of the high-order spectrum of the previous interference fringe is multiplied by the high-order spectrum of the subsequent fringe to calculate the phase difference for calibrating half-wave voltage.

Methods We adopt the phase angle of the cross-correlation function between multiple fringe images to determine the phase difference. After converting the fringe illumination light to the frequency domain, the high-order spectrum is extracted. In the spectra of multiple fringe patterns, the conjugate of the high-order spectrum of the previous one is multiplied by the next one to obtain the cross-correlation function of adjacent images. The angle of this function is the phase difference between two fringe images. The feasibility of this method is verified by generating fringe images with the same phase difference in Matlab. The optical path for experimental calibration is part of a structured illumination super-resolution microscopy system. This system achieves high-speed imaging based on electro-optic modulators and galvanometers. One optical path passes through a phase electro-optic modulator, while the other does not. Finally, the two beams interfere at the camera through a mirror to form fringes.

Results and Discussions The experiment applies voltage to the EOM through a computer-controlled acquisition card, with a voltage interval of 1 V and a voltage range of −10 V to 9 V. When the voltage is changed each time, the camera is controlled to acquire an image and save it. A total of 20 interference fringe images with equal interval displacement are collected. The 640 nm and 561 nm lasers are utilized for calibration, and the calibration results of the Michelson interferometry method serve as the correct results for accuracy consideration. To further eliminate the errors caused by interference, we take nine sets of fringe images for each laser wavelength, calculate the average value of the nine sets of results, and then compare this value with the accurate calibration value. The half-wave voltage obtained by calibrating the 640 nm using the Michelson interferometry method is 6.6 V, and the result obtained using this method is 6.57 V, with a difference of 0.03 V and an error of 0.45%. The half-wave voltage obtained by calibrating the 561 nm using the Michelson interferometry method is 5.87 V, and the result obtained by this method is 5.84 V, with a difference of 0.03 V and an error of 0.51%. After converting to phase difference, the phase difference calculated for 640 nm is 0.478 rad, the standard phase difference is 0.476 rad, and the difference is 0.002 rad. The phase difference calculated for 561 nm is 0.538 rad, the standard phase difference is 0.535 rad, and the difference is 0.003 rad. By employing the contour method

to process the 640 nm image, the obtained half-wave voltage is 6 V, which has a larger error than the result obtained by this method. The half-wave voltage obtained by our method is close to that obtained by the Michelson interferometry method, with the same accuracy and faster speed.

Conclusions Before adopting an electro-optic modulator, it is often necessary to calibrate the half-wave voltage. Previous methods such as Michelson interferometry require additional optical path construction, and the calibration process is slow and easily interfered by noise and jitter. Thus, the contour method is not accurate enough. Therefore, a method based on the high-order cross-correlation of the interference fringe frequency domain is proposed to calculate the phase difference between fringe images and calibrate the half-wave voltage of the electro-optic modulator. This method employs a specific mask to remove the 0th-order spectrum and extract the high-order spectrum. The complex conjugate of the high-order spectrum of the previous image is multiplied by the high-order spectrum of the next image to obtain the angle and then solve for the phase difference. The phase error in actual detection reaches 0.002 rad and the half-wave voltage error is 0.03 V, which meet the calibration requirements of electro-optic modulators. Since the proposed method has a large calibration speed and does not require optical path rebuilding, it can check whether the electro-optic modulator drifts at any time and whether corrections are needed or not.

Key words Fourier optics; signal processing; spectrum analysis; phase conjugation; cross-correlation; electro-optic modulator